International Journal of Applied Mathematics Electronics and Computers

ISSN:2147-8228 http://dergipark.gov.tr/ijamec Original Research Paper

Real-Time Speed Control of BLDC Motor Using Adaptive Fuzzy Fractional Sliding Mode Controller

Kamil Orman*[1]

Accepted : 18/12/2018 Published: 26/12/2018 **DOI: 10.18100/ ijamec.2018447370**

Abstract: In this study, a fractional order sliding mode controller (FOSMC) and adaptive fuzzy fractional order sliding mode controller (AFFOSMC) are designed for speed control of the Brushless DC motor and the performance of the controllers have been tested in real time. Experimental studies were performed to compare the performance of the reference tracking and error elimination of both controllers, and the graphs of the results were presented.

Keywords: *BLDC motor, Fractional sliding mode control, Adaptive fuzzy fractional sliding mode control, Speed control*

1. Introduction

BLDC motors are widely used in many areas of industry, especially in applications requiring speed and position control. Due to the nonlinear structure of systems that perform speed and position control using BLDC motors, control is difficult. The controllers designed for this reason are required to respond to this difficulty and need to work efficiently. There are many studies in the literature for speed control of BLDC motors. Yu and Rey-Chue used LQR method to find the optimum parameters of PID speed controller [1]. Sathyan et al. introduced a new digital control concept for BLDC motors and developed a low-cost controller for inefficient single-phase induction motors. Also under dynamic load conditions, the proposed controller was indicated to be capable of regulating speed without the use of an observer [2]. Liu et al. presented a control system with a new speed estimation approach based on model reference adaptive control (MRAC) for low cost brushless dc motor drives with low resolution hall sensor [3]. In the proposed method, a speed estimation algorithm based on MRAC was used to correct the speed error calculated using EMF. Ahmed et al. [4] they have compared PI speed controller and fuzzy PI speed controller performance in their simulation studies. They also stated that the performance of the fuzzy PI controller is generally better than the PI speed controller. In the simulation work presented by Mulljik [5], it was stated that BLDC's speed control using Fuzzy Logic Controller has a better performance than PI and PID controllers. Kumari et al. presented a Genetic Algorithm (GA) based design of a PID controller for the speed control of a BLDC motor [6].

In real dynamical systems, sliding mode control method, which has the ability to remove the effects of uncertainties caused by model errors and undesirable disturbing effects that affect the system response, has been widely used and modified. Choi et al. [7] proposed Global SMC to control second-order time-varying systems with parameter uncertainties and disruptive effects. The proposed controller has applied to the BLDC motor with indeterminate loads. Experimental results of the proposed controller are very similar to the results of the simulated and closed form equation and they show that best performance compared to other SMCs. In [8], an SMC-fuzzy speed control approach is proposed. A constantly changing term is used instead of the "sgn" function to remove the effect of the chattering. A fuzzy control term has been used to improve the dynamic response of the system and to reduce the steady state error in the boundary layer. Experimental results, compared with the results of conventional PID, confirm that the proposed sliding mode controller can provide good tracking performance and is robust against uncertainties and disturbances. To test the speed of an electromechanical system, Eker İ. was tested a sliding-mode control approach that is described in the form of sliding surface 'PID' [9]. It has also been noted that the chattering effect is exceeded by using a hyperbolic function for the sliding surface. Xiaojuan and Liu[10] introduced a new adaptive fuzzy sliding mode control approach. Two types of sliding mode control methods have been used in their work, which are based on equivalent control and based on the reaching phase of the AFSMC algorithm. It is also stated that the output value of the sliding mode controller is changed according to the value range of the switching function and the system stability is improved by removing the chattering effect. Simulation results comparing the fuzzy sliding mode control scheme to show the effectiveness of the proposed structure and the improvement of the dynamic performance of the system are given. Wang et al. proposed Hybrid terminal sliding mode control method for sensorless position control of an electric vehicle using a brushless DC motor [11]. In the method they used, the back EMF sensing approach were analyzed and improved. Improvement efforts have not only removed the chattering effect of a zero crossing signal but also it was improved reliability and stability. The dynamic performance of the proposed structure was tested with experimental results and efficiency was shown in terms of stability and energy saving.

In this study, a BLDC motor was tested for speed control for low and medium speeds. Fractional order sliding mode control and adaptive fuzzy fractional order sliding mode control methods are applied separately. Experimental results show that the adaptive fuzzy fractional sliding mode controller has better performance than the fractional sliding mode control.

[1] *Department of Computer Engineering, Faculty of Engineering, Erzincan University, TURKEY*

** Corresponding Author: Email: korman@erzincan.edu.tr*

2. BLDC Motor Model

Taking into account the DC motor equations, the transfer function of the BLDC motor is obtained. DC motor voltage equations can be expressed as follows.

$$V = L\frac{di}{dt} + iR + E \tag{1}$$

$$E = K_e \frac{d\varphi}{dt} \tag{2}$$

If Eq. (2) is substituted in Eq. (1) and the current expression is denoted by Eq. (1);

$$L\frac{di}{dt} = V - iR - K_e\frac{d\varphi}{dt} \tag{3}$$

is obtained. The expression of the mechanical part of the BLDC motor;

$$iK_t = J_m\frac{d^2\varphi}{dt^2} + B_m\frac{d\varphi}{dt} \tag{4}$$

and, If equation (3) and equation (4) are rewritten in s-form to obtain the transfer function,

$$LsI(s) = V(s) - RI(s) - K_e s\varphi(s) \tag{5}$$

$$KtI(s) = J_m s^2\varphi(s) + B_m s\varphi(s) \tag{6}$$

and if equation (5) is rearranged to obtain I(s)

$$I(s) = \frac{V(s) - K_e s\varphi(s)}{R + Ls} \tag{7}$$

is obtained. Using this equation in Eq. (6)

$$\frac{K_t[V(s) - K_e s\varphi(s)]}{R + Ls} = J_m s^2\varphi(s) + B_m s\varphi(s) \tag{8}$$

$$K_t V(s) - K_t K_e s\varphi(s) = \varphi(s)[J_m s^2 + B_m s][R + Ls] \tag{9}$$

$$V(s) = \frac{\varphi(s)[J_m s^2 + B_m s][R + Ls] + K_t K_e s\varphi(s)}{K_t} \tag{10}$$

$$s\frac{\varphi(s)}{V(s)} = \frac{Kt}{[J_m s + B_m][R + Ls] + K_t K_e} \tag{11}$$

is obtained. If equation (11) is rewritten using $s\varphi(s) = \omega(s)$

$$\frac{\omega(s)}{V(s)} = \frac{K_t}{[J_m s + B_m][R + Ls] + K_t K_e} \tag{12}$$

The expression is obtained. Thus, the transfer function of the DC motor can be written as follows.

$$G(s) = \frac{\omega(s)}{V(s)} = \frac{K_t}{LJ_m s^2 + (J_m R + B_m L)s + RB_m + K_t K_e} \tag{13}$$

Equation (13) is simplified under the following assumptions,

1. B_m tends to go too small and even zero,
2. $J_m R >> B_m L$
3. $K_t K_e >> RB_m$

and very small values are neglected, the transfer function expressed in Eq. (13) can be written as in Eq. (14).

$$G(s) = \frac{K_t}{LJ_m s^2 + J_m Rs + K_t K_e} \tag{14}$$

Eq. (14) is multiplied by the following expression,

$$\frac{R}{K_t K_e} * \frac{1}{R}$$

and the transfer function is rewritten;

$$G(s) = \frac{\frac{1}{K_e}}{\frac{RJ_m}{K_t K_e}\frac{L}{R}s^2 + \frac{RJ_m}{K_t K_e}s + 1} \tag{15}$$

is obtained. Where *'K_t'* is torque constant (*mNm/A*), *'K_e'* is electrical torque (*Vsec/rad*), *'B_m'* is friction coefficient (*Nm/(rad/sec)*), *'R'* is resistance between phases (Ω), *'L'* phase inductance (mH) and *'J_m'* motor inertia (*Kgm*^{2}).
Mechanical and the electrical time constants;

$$\tau_m = \frac{RJ_m}{K_t K_e}\ ,\ \tau_e = \frac{L}{R} \tag{16}$$

if the expressions are written in Eq. (15)

$$G(s) = \frac{\frac{1}{K_e}}{\tau_m\tau_e s^2 + \tau_m s + 1} \tag{17}$$

equality is achieved. Equations (16) show the difference between DC motor and BLDC motor. The mechanical and electrical time constants in the motor model are very important.

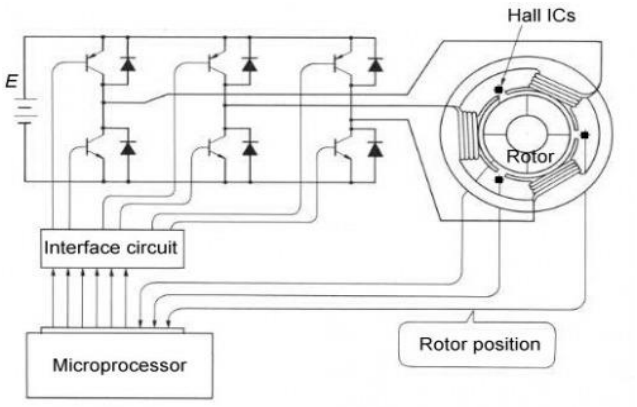

Figure 1. Typical BLDC Motor drive

From the symmetrical structure of BLDC motor shown in fig.1, Eq. (16) is obtained as follows.

$$\tau_m = \sum\frac{RJ_m}{K_t K_e} = \frac{J_m\sum R}{K_t K_e} \tag{18}$$

Since there are 3 phases in symmetrical structure, mechanical and electrical constants;

$$\tau_m = \frac{J_m 3R}{K_t K_e}\ ,\quad \tau_e = \frac{L}{3R} \tag{19}$$

It is specified by the equations. In addition, the relationship between electrical and mechanical torques can be expressed by

using the electric energy and mechanical power equations as follows:

$$\sqrt{3} * E * I = \frac{2\pi}{60} * N * T \quad (20)$$

$$\frac{E}{N} = \frac{T}{I} * \frac{2\pi}{60\sqrt{3}} \quad (21)$$

$$K_e = K_t * \frac{2\pi}{60\sqrt{3}} = K_t * 0.0605 \quad (22)$$

2.1. Brushless DC motor (Maxon motor - EC 32)

The mathematical model of the BLDC motor was obtained according to the values given in Tables 1 and 2. K_e, τ_m and τ_e values require calculation.

Table 1: Maxon BLDC motor operation features [12]

S. No.	Parameter (unit)	Specification
1	Nominal voltage - V	24
2	No load speed - rpm	11000
3	No load current - mA	286
4	Nominal speed - rpm	9510
5	Nominal torque - mNm	43.6
6	Nominal current - A	3.37
7	Stall torque - mNm	355
8	Starting current - A	17.3
9	Maximum efficiency	76%

Table 2: Characteristic features of Maxon BLDC motor [12]

S. No.	Parameter (unit)	Specification
1	Terminal resistance phase to phase - Ω	1.39
2	Terminal inductance phase to phase - *mH*	0.226
3	Torque constant - *mNm/A*	20.5
4	Speed constant - *rpm/V*	465
5	Speed/torque gradient - *rpm/mNm*	31.5
6	Mechanical time constant - *ms*	6.59
7	Rotor inertia- gcm^2	20

If the following calculations are made according to the values given above;

$$\tau_e = \frac{L}{3R} = \frac{0.226 * 10^{-3}}{3 * 1.39} = 54.19 * 10^{-6} \quad (23)$$

$$\tau_m = \frac{J_m 3R}{K_t K_e} = 0.00659 s \quad (24)$$

$$K_e = \frac{J_m 3R}{K_t \tau_m} = \frac{2 * 10^{-6} * 3 * 1.39}{20.5 * 10^{-3} * 0.00659} = 0.06173 \quad Vsec/rad \quad (25)$$

These values are substituted in Eq. (17) and G (s) is obtained as follows.

$$G(s) = \frac{\frac{1}{0.06173}}{0.00659 * 54.19 * 10^{-6} * s^2 + 0.00659 * s + 1} \quad (26)$$

$$G(s) = \frac{16.19}{0.357 * 10^{-6} * s^2 + 0.00659 * s + 1} \quad (27)$$

Equation (27) indicates the transfer function of the BLDC motor used.

3. Control

In this section, the mathematical equations designed controllers and their block diagrams are given.

3.1. Sliding Mode Control

The system controlled by the sliding mode controller and the error signal can be defined as follows;

$$m\ddot{x}(t) + b\dot{x}(t) + kx(t) = u \quad (28)$$
$$\varepsilon(t) = x_{ref}(t) - x(t) \quad (29)$$

If this system given from the second order is transformed into a first order system with $\dot{x} = v$ transformation;

$$\ddot{x} = \dot{v} = \frac{1}{m}(u - bv - kx) \quad (30)$$
$$\begin{bmatrix} \dot{x} \\ \dot{v} \end{bmatrix} = \begin{bmatrix} 0 & 1 \\ \frac{-k}{m} & \frac{-b}{m} \end{bmatrix} \begin{bmatrix} x \\ v \end{bmatrix} + \begin{bmatrix} 0 \\ \frac{1}{m} \end{bmatrix} u \quad (31)$$

If the sliding surface is defined as follows:

$$s = \{x : \sigma(x, t) = 0\} \quad (32)$$

and the sliding function (σ) can be determined as follows,

$$\sigma = G(x_{ref} - x) = G\varepsilon = \phi(t) - \varphi(x) \quad (33)$$

$$\left.\begin{aligned} \phi(t) &= Gx_{ref} \\ \varphi(x) &= Gx \\ \frac{d\varphi(x)}{dx} &= G \end{aligned}\right\} \quad (34)$$

The solution to be obtained if the sliding function is derived and equated to zero is called the equivalent control. If the derivative of the equation (33);

$$\frac{d\sigma}{dt} = \frac{d\phi(t)}{dt} - \frac{d\varphi(x)}{dx}\frac{dx}{dt} \quad (35)$$

is obtained.

$$\frac{dx}{dt} = \dot{x} = f(x, t) + Bu \quad (36)$$

If Equation (34) and Equation (36) are written in Equation (35);

$$\frac{d\sigma}{dt} = \frac{d\phi(t)}{dt} - G(f(x, t) + Bu) \quad (37)$$

The ($u = u_{eq}$) value, which makes the equation (37) zero, is equal to the equivalent control.

$$\left.\frac{d\sigma}{dt}\right|_{u=u_{eq}} = \frac{d\phi(t)}{dt} - G(f(x, t) + Bu_{eq}) = 0 \quad (38)$$

$$GBu_{eq} = \frac{d\phi(t)}{dt} - G(f(x, t) \quad (39)$$

If a Lyapunov function is selected as follows;

$$V = \frac{1}{2}\sigma^T\sigma > 0 \quad \text{and} \quad \dot{V} = \sigma^T\dot{\sigma} \quad (40)$$

for stability;

$$\dot{V} = -\sigma^T D\sigma < 0 \tag{41}$$

and if the derivatives in Equation (40) and Equation (41) are equalized,

$$\sigma^T \dot{\sigma} = -\sigma^T D\sigma \tag{42}$$

In the solution of this equation

$$\dot{\sigma} + D\sigma = 0 \tag{43}$$

is obtained. Here (D) determines the speed of approach of the system states to the sliding surface.
If $(\dot{\sigma})$ in Equation (35) is replaced by Equation (43) to obtain the control signal,

$$\frac{d\phi(t)}{dt} - G(f(x,t) + Bu) + D\sigma = 0 \tag{44}$$

If Equation (44) is rewritten using Equation (39);

$$GBu_{eq} - GBu + D\sigma = 0 \tag{45}$$

As a result of a short mathematical operation, the control signal is obtained as follows.

$$u = u_{eq} + K\sigma \tag{46}$$

where $K = (GB)^{-1}$. In this way, the effect of the chattering in the system will be removed by adding the $(K\sigma)$ sign, which is a continuous sign to the equivalent control signal (u_{eq}). However, to eliminate the difficulties that may arise during the calculation of the equivalent control expression (u_{eq}) the equivalent controller estimate can be used instead of the equivalent control expression (u_{eq}).

If the matrices of $f(x,t)$ and B in the equivalent controller equation expressed by Eq. (39) are not known at all, or if little is known, it is impossible to calculate (u_{eq})or will be very different from real (u_{eq}). For the estimation of (u_{eq}); moving from the physical meaning of the effect of the equivalent controller, it can be said that the equivalent control is the average value of the total control. In this case, the equivalent control would be appropriate to design with a low pass filter which determines the average of the entire signal instead of the rapidly varying high frequency components in the total control signal.

$$u = u_{eq} + \Delta u + K\sigma \tag{47}$$

Where u_{eq} is the component of the mean value of the total control signal and Δu is the high frequency component of the total control signal.
In this case a filter such as the following can be designed for the estimated equivalent controller $(\hat{u}_{eq})$.

$$\hat{u} = \hat{u}_{eq} + \tau\hat{u}_{eq} \quad \text{and} \quad \hat{u}_{eq} = \frac{1}{1+\tau s}u \tag{48}$$

where $1/\tau$ denotes the value of the cut-off frequency of the filter. The main purpose of a low-pass filter design is that the characteristics of a control system are determined by low-frequency components. High frequency components come from generally modeled components.
If Equations (48) are rewritten using Equations (46) in the light of these definitions,

$$u = \hat{u}_{eq} + K\sigma \ , \qquad u = \frac{1}{1+\tau s}u + K\sigma \tag{49}$$

it is necessary to check the speed of error and error in order to obtain a robust control. In this case (σ) can be determined as follows.

$$\sigma = \dot{\varepsilon} + G\varepsilon \tag{50}$$

By substituting Equation (50) in Equation (49), the control signal of the sliding mode control (SMC) obtained as follows.

$$u = \frac{1}{1+\tau s}u + K(\dot{\varepsilon} + G\varepsilon) \tag{51}$$

3.2. Fractional Order Sliding Mode Control

Fractional calculation is a generalization of derivatives and integrals with a notation such as ${}_aD_t^p$ for non-integer parts. The continuous integro-differential definition of this notation is as follows.

$${}_aD_t^p = \begin{cases} \dfrac{d^p}{dt^p} & : p > 0 \\ 1 & : p = 0 \\ \displaystyle\int_a^t (d\tau)^{-p} & : p < 0 \end{cases} \tag{52}$$

In this notation, *a* and *t* are the bounds of the operation and $p \in R$. There are several mathematical definitions for fractional derivative and integral [13],[14]. Among these definitions, the definition of Grünwald-Letnikov (GL) and the definition of Riemann-Liouville (RL) are more widely used. The definition of GL is as follows;

$${}_aD_t^p f(t) = \lim_{h \to 0} h^{-p} \sum_{j=0}^{\left[\frac{t-a}{h}\right]} (-1)^j \binom{p}{j} f(t - jh) \tag{53}$$

In the equation, [.] Refers to the integer part, and the RL definition is as follows. (n-1 <p <n);

$${}_aD_t^p f(t) = \frac{1}{\Gamma(n-p)} \frac{d^n}{dt^n} \int_a^t \frac{f(\tau)}{(t-\tau)^{p-n+1}} d\tau \tag{54}$$

In equation, Γ(.) represents the Euler gamma function. If the sliding mode control signal obtained from Equation (51) is written as follows using fractional calculation,

$$u = \frac{1}{1+\tau s}u + K({}_aD_t^p \varepsilon + G\varepsilon) \tag{55}$$

the control signal of the fractional order sliding mode control is obtained in this way.

3.3. Adaptive Fuzzy Fractional Order Sliding Mode Control

The design parameter (G) defined in Equation (34) must have an optimum value. The inputs of the fuzzy identification algorithm are (ε) and (ε̇). The membership value are determined according to the Fuzzy sets. $\hat{G}_f(k+1)$ will be calculated using these

membership values based on how much (G_f) needs to increase or decrease. At the last stage, $\hat{G}_f(k+1)$ will be calculated by an adaptation law and an adaptive fuzzy fractional order sliding mode controller (AFFOSMC), which is the final control approach, will be obtained. The parameters of the fuzzy identifier are set using a recursive least square (RLS) recursive method. The block diagram of the adaptive fuzzy fractional order sliding mode controller is given in Fig.2

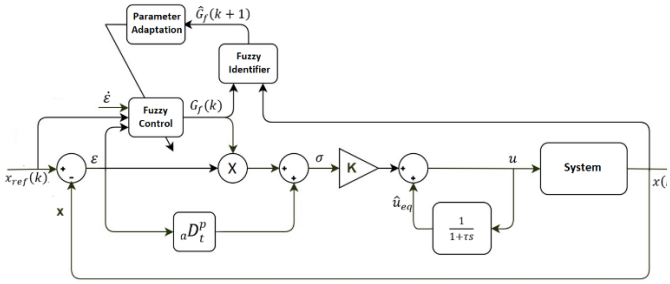

Figure 2. Structure of Adaptive fuzzy fractional order sliding mode control (AFFOSMC)

The table of rules for the designed fuzzy controller is as in Table 3 and the membership functions of the inputs are given in Table 4.

Table 3: Fuzzy Logic Rule Table

ε/ε̇	NB	NM	NS	Z	PS	PM	PB
NB	7	7	7	6	6	5	4
NM	7	7	6	6	5	4	3
NS	7	6	6	5	4	3	2
Z	6	6	5	4	3	2	2
PS	6	5	4	3	2	2	1
PM	5	4	3	2	2	1	1
PB	4	3	2	2	1	1	1

Note: The numbers in the table indicate the rule numbers.

Table 4: Memberships function for ε and ε̇

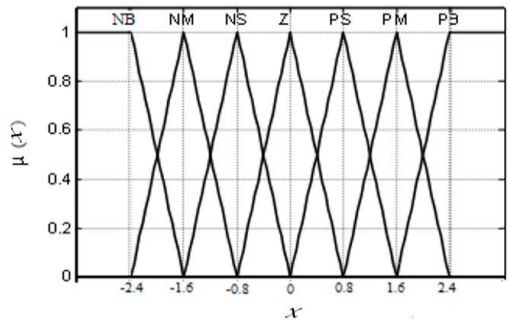

i th rule that determines the output function of identifier model is;

$$IF\ \ x(k) = \tilde{A}^i \text{ Then } \hat{G}_{fi}(k+1) = a_i x(k) + b_i G_f(k) \quad (56)$$

Where $x(k)$ is the system output and $G_f(k)$ is the fuzzy design parameter. a_i and b_i $(i = 1,2,\dots,R)$ are the parameters of the results. $\tilde{A}^i$ is linguistic value, $\hat{G}_{fi}(k+1)$ identifier model output for only rule i. By using Center-Average Defuzzification, the following descriptive model output is obtained:

$$\hat{G}_{fi}(k+1) = \frac{\sum_{i=1}^{R} \hat{G}_{fi}(k+1)\,\mu_i}{\sum_{i=1}^{R} \mu_i} \quad (57)$$

In order to simplify this expression, the following definition is made.

$$\lambda_i = \frac{\mu_i}{\sum_{i=1}^{R} \mu_i} \quad (58)$$

Then general model;

$$\hat{G}_f(k+1) = \sigma^T \lambda \quad (59)$$

where $\hat{G}_f(k+1)$ is the identifier model output. σ and λ are defined as,

$$\sigma = [a_i \dots a_R\ b_i \dots b_R]^T \quad (60)$$

$$\lambda = \left[x(k)\lambda_i \dots x(k)\lambda_R\ \ G_f(k)\lambda_i \dots G_f(k)\lambda_R\right]^T \quad (61)$$

The RLS algorithm and update formula are given below.

$$g(k) = P(k)\lambda[\rho I + \lambda^T P(k)\lambda]^{-1} \quad (62)$$

$$P(k+1) = \left(1/\rho\right)(I - g(k)\lambda^T)P(k) \quad (63)$$

$$\sigma(k+1) = \sigma(k) + g(k)(x(k+1) - \lambda^T \sigma(k)) \quad (64)$$

If the rule of Equation (56) is rewritten;

$$\text{IF } x(k) = \tilde{A}^i \text{ Then } G_{fi}(k) = k_{1i} x_{ref}(k) - k_{2i} x(k) \quad (65)$$

Where $G_{fi}(k)$ is the identifier model output for only rule i. Our controllers that are tuned are given by,

$$G_f(k+1) = \frac{\sum_{i=1}^{R} G_{fi}(k+1)\,\mu_i}{\sum_{i=1}^{R} \mu_i} \quad (66)$$

where, the certainty of the premise membership function for a rule implies the certainty of the membership function because of the existence of a single entry.

$$\mu_i\big(x(k)\big) = \mu\big(x(k)\big) \quad (67)$$

For the fuzzy controller a certainty equivalence approach is used. If the system operates according to the *i.th* rule and there is little or no influence from the other rules, then $x(k) = x_i(k)$.
As a result, the following equation is achieved.

$$\hat{G}_{fi}(k) = G_{fi}(k+1) = a_i b_i(k) + b_i\left[k_{1i} x_{ref}(k) - k_{2i} x_i(k)\right] \quad (68)$$

If we choose k_{1i} and k_{2i} for $i = 1,2,\dots,R$, then the pole of the closed loop system is at 0.1 and the steady state error between $x_{ref}(k)$ and x(k)becomes zero. If the z-transforms of $x_i(k)$ and $x_{ref}(k)$ are $X_i(k)$ and $X_{ref}(k)$ respectively,

$$\frac{X_i(z)}{X_{ref}(z)} = \frac{b_i k_{1i}}{z + b_i k_{2i} - a_i} \quad (69)$$

The indirect adaptive scheme to be used for the controller can be determined as follows.

$$k_{2i} = \frac{a_i - 0.1}{b_i} \quad (70)$$

Here, for each $i = 1,2, \ldots, R$, the a_i and b_i estimates determined by the identifier are used. In order to make the steady state error zero, k must be large and $G_{fi}(k+1) = G_{fi}(k)$ and $x_i(k+1) = x_i(k) = x_{ref}(k)$ for *(i = 1,2, ..., R)*. From Equation (68);

$$k_{1i} = \frac{0.1 - a_i + b_i k_{2i}}{b_i} \quad (71)$$

Equation (70) and Equation (71) can be used to design a controller that includes an indirect adaptive scheme. a_i and b_i for each *i.* will be determined by the identifier and k_{1i} and k_{2i} will be updated for each *i*.

4. Experimental Result

In this section, the controllers are compared in terms of the rise time, reference tracking and the ability to reduce the error. The square and trapezoidal speed references for the speed control of the BLDC motor are used and the experimental results are given in Figures 3-10. In the first experimental study, 10 rpm square speed reference is chosen for testing FOSMC and AFFOSMC. As shown in Fig. 3 and Fig.5, FOSMC has a faster rise time than the AFFOSMC at the start of BLDC motor movement.

However, when the square reference changes to the ±10 Rpm, AFFOSMC gives fast rise time and less overshoot. In addition, the AFFOSMC has performed better than the FOSMC in terms of reference tracking.

The results for square speed reference at 1000 rpm are given in Fig. 4 and Fig. 6. The rise time of the AFFOSMC for this reference is approximately 0.5 seconds. FOSMC's rise time is approximately 1.5 seconds and with having less overshoot.

In the second experimental study, the trapeze speed reference with slow changes was chosen and the experimental results are given in Figure 7-10. As shown in Fig. 7 and Fig. 9, the AFFOSMC has a better rise time than the FOSMC for 10 rpm trapeze speed reference and is more successful in tracking the reference. In addition, the FOSMC controller has overshoot.

Finally, the results for the 1000 rpm trapeze speed reference are given in Fig.8 and Fig.10. Although they have similar performance in terms of reference tracking, the AFFOSMC is faster than the FOSMC controller in terms of rise time.

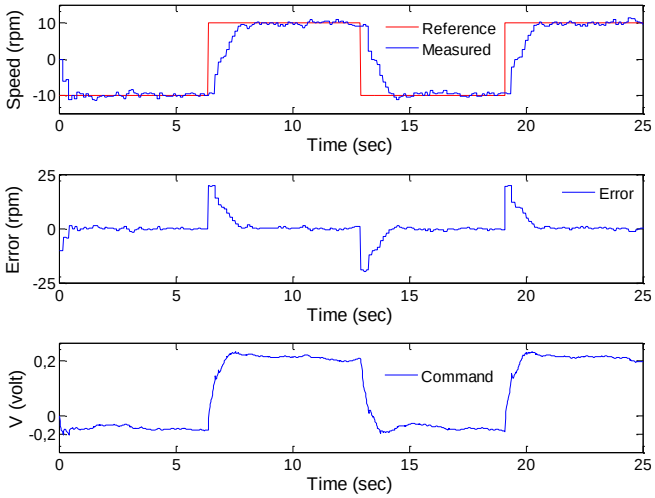

Figure 3. Fractional order sliding mode 10 rpm square ref.

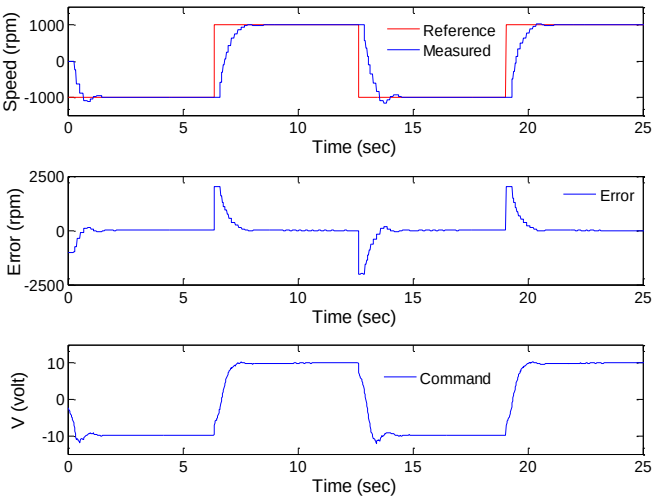

Figure 4. Fractional order sliding mode 1000 rpm square ref.

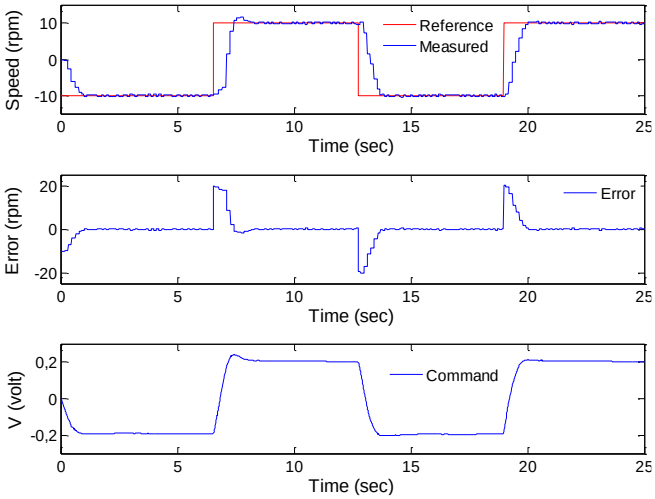

Figure 5. Adaptive fuzzy fractional order sliding mode 10 rpm square ref.

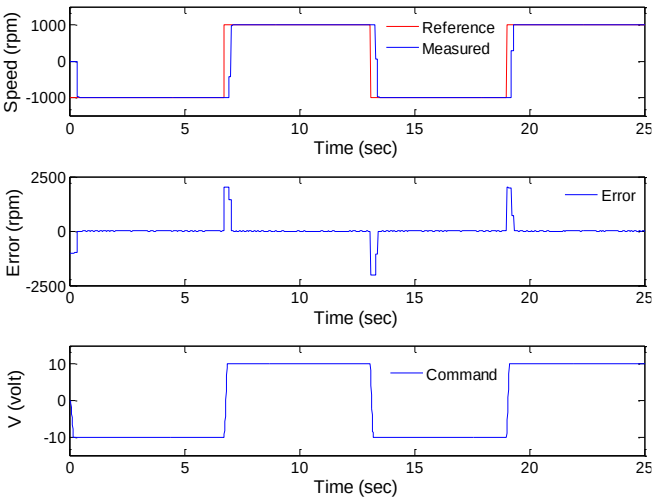

Figure 6. Adaptive fuzzy fractional order sliding mode 1000 rpm square ref.

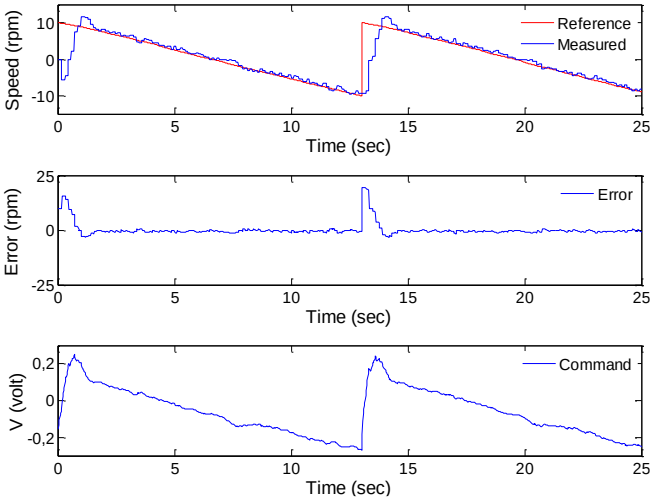

Figure 7. Fractional order sliding mode 10 rpm trapeze ref.

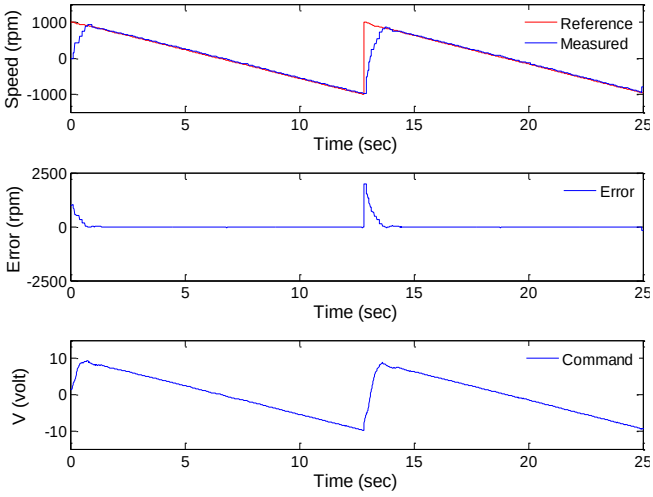

Figure 8. Fractional order sliding mode 1000 rpm trapeze ref.

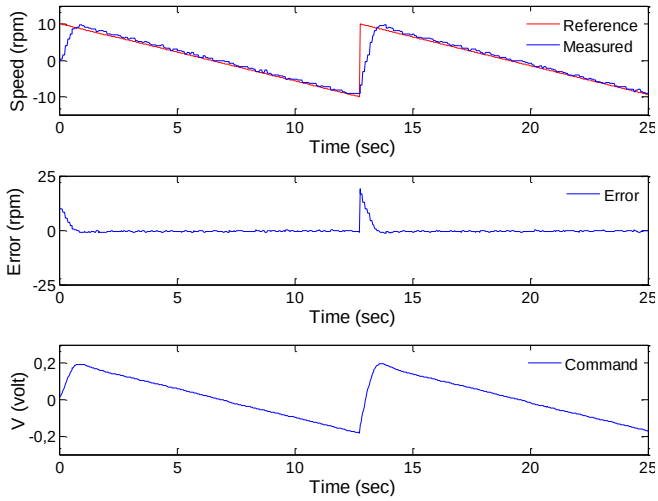

Figure 9. Adaptive fuzzy fractional order sliding mode 10 rpm trapeze ref.

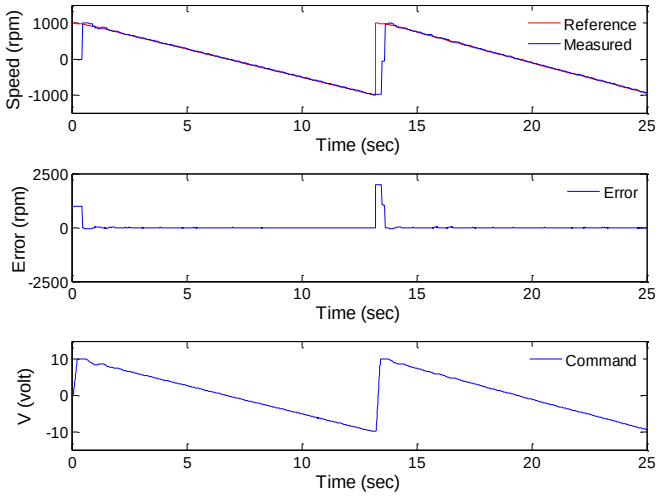

Figure 10. Adaptive fuzzy fractional order sliding mode 1000 rpm trapeze ref.

5. Conclusions

In this study, an adaptive fuzzy fractional order sliding mode controller was tested for the speed control of the brushless DC motor and the experimental results are presented.

The experimental results show that the AFFOSMC shows better performance with smaller speed error, better rise time and reference tracking when it compared to the responses of FOSMC.

References

[1] Yu, Gwo-Ruey, and Rey-Chue Hwang. "Optimal PID speed control of brush less DC motors using LQR approach." Systems, Man and Cybernetics, 2004 IEEE International Conference on. Vol. 1. IEEE,

[2] Sathyan, Anand, et al. "An FPGA-based novel digital PWM control scheme for BLDC motor drives." IEEE transactions on industrial electronics 56.8 (2009): 3040-3049.

[3] Liu, Yang, et al. "Model reference adaptive control-based speed control

[4] of brushless DC motors with low-resolution Hall-effect sensors." IEEE

[5] Transactions on Power Electronics 29.3 (2014): 1514-1522.

[6] Ahmed M., et al. "Brushless DC motor speed control using both PI controller and fuzzy PI controller." International Journal of Computer Applications 109.10 (2015): 29-35.

[7] Mullick, Jahir Abbas. "Fuzzy Controller for Speed Control of BLDC motor using MATLAB." (2017).

[8] Kumari, Swati, et al. "GA Based Design of Current Conveyor PLD Controller for the Speed Control of BLDC Motor." 2018 4th International Conference on Computational Intelligence & Communication Technology (CICT). IEEE, 2018.

[9] Choi, Hyeung-sik, et al.2001 "Global sliding-mode control. Improved design for a brushless DC motor." IEEE Control Systems 21.3:27-35.

[10] Song, Hailong, et al. "A novel SMC-fuzzy speed controller for permanent magnet brushless DC motor." Applied Power Electronics Conference and Exposition, 2003. APEC'03. Eighteenth Annual IEEE. Vol. 1. IEEE, 2003.

[11] Eker, Ilyas. "Sliding mode control with PID sliding surface and experimental application to an electromechanical plant." ISA transactions 45.1 (2006): 109-118.

[12] Xiaojuan, Yan, and Liu Jinglin. "A novel sliding mode control for BLDC motor network control system." Advanced Computer Theory and Engineering (ICACTE), 2010 3rd International Conference on. Vol. 2. IEEE, 2010.

[13] Wang, Yaonan, et al. "Position-sensorless hybrid sliding-mode control of electric vehicles with brushless DC motor." IEEE

transactions on vehicular technology 60.2 (2011): 421-432.
[14] https://www.maxonmotor.com/medias/sys_master/root/8825424085022/17-EN-218.pdf
[15] Oldham, K.B. and Spanier, J. The Fractional Calculus, Academic Press, 1974.
[16] I. Podlubny, Fractional Differential Equations, Academic Press, San Diego, California, 1999.